RESEARCH ARTICLE

Evaluation of the Characteristics of Congenital Portosystemic Shunts in Dogs and Cats Using Computerised Tomography Angiography and Brain Magnetic Resonance Imaging [1]

Yağmur KOÇAK [1] (ID) Zihni MUTLU [2] (ID) Murat KARABAĞLI [2] (ID) Yusuf ALTUNDAĞ [2] (*) (ID)
Berjan DEMİRTAŞ [3] (ID)

[1] This study was presented as an oral presentation at the 17th national 3rd international veterinary surgery congress held in Samsun, Türkiye on 17 September 2022.

[1] Istanbul Üniversitesi-Cerrahpaşa, Institute of Graduate Studies, TR-34315 İstanbul - TÜRKİYE
[2] Istanbul University-Cerrahpasa, Faculty of Veterinary Medicine, Surgery Department, TR-34315 İstanbul - TÜRKİYE
[3] İstanbul University-Cerrahpaşa, Vocational School of Veterinary Medicine, Department of Plant and Animal Production, Equine and Training Programme, TR-34315 İstanbul - TÜRKİYE

(*) **Corresponding author:** Yusuf ALTUNDAĞ

Phone: +90 212 866 3700
Cellular phone: +90 506 398 8801
Fax: +90 212 866 3851
E-mail: ysf.altundag@hotmail.com

Abstract

Portosystemic shunts (PSS) are abnormal vessels that allow blood to bypass the liver, leading to a variety of clinical symptoms due to the lack of normal hepatic metabolism. Imaging modalities like Computed Tomography Angiography (CTA) and Magnetic Resonance Imaging (MRI) are critical in the diagnosis and characterization of PSS. Nine animals, with clinical presentations suggestive of CPSS, underwent CTA and brain MRI. The CTA was performed using a 32-detector CT unit, and MRI scans were conducted on a 1.5 Tesla Siemens Magnetom Avanto system. Six cases of extrahepatic portosystemic shunts (EPSS) and three intrahepatic shunts (IHPSS) were diagnosed. MRI findings included brain atrophy and white matter hyperintensities, correlating with the type of shunt. The study demonstrates the value of MRI in identifying specific brain changes associated with CPSS. Advanced imaging techniques are indispensable for the accurate diagnosis of CPSS. The study's findings reinforce the need for further research with a larger cohort to establish a stronger correlation between CPSS types and brain MRI changes, aiming to enhance clinical management for affected animals.

Keywords: Cat, Computed tomography, Congenital portosystemic shunt, Dog, Magnetic resonance imaging

INTRODUCTION

Portosystemic shunts (PSS) are congenital vascular anomalies that allow the direct passage of portal venous blood into the systemic circulation [1]. There are two main forms: intrahepatic portosystemic shunts (IHPSS) and extrahepatic portosystemic shunts (EHPSS). IHPSS typically originates from the left branch of the portal vein and is associated with the failure of the closure of the ductus venosus. EHPSS, on the other hand originate from a part of portal system which is outside the liver [2-4].

Congenital portosystemic shunts (CPSS) lead to bypass of the ammonia-rich blood away from the liver, and this condition is the most common cause of the hepatic encephalopathy (HE) in cats and dogs [5]. Clinical symptoms of HE include mental alterations, seizure activities, and proprioceptive deficiencies [6]. These symptoms may become more pronounced after the consumption of high-protein foods [7].

It is well known that ammonia is only metabolized in the astrocytes of the brain [8,9]. Astrocytes produce glutamine by the metabolization of ammonia and glutamate by an enzyme called glutamine synthetase which is found in the endoplasmic reticulum of astrocytes [10]. However, in cases of liver failure, increased ammonia levels elevate

the intracellular glutamine level [11,12]. Mitochondrial dysfunction, the formation of "Alzheimer type II astroglia," and changes in cerebral metabolism may occur as a result of this process [8,10].

Computed Tomography Angiography (CTA) has emerged as a more advantageous tool for the diagnosis of PSS in dogs compared to other methods [13]. Advances in Multidetector Computed Tomography (MD-CT) technology have reduced the examination time and the doses of radiation which make computed tomography (CT) more widely used in liver assessments [14]. The progress in MD-CT technology allows for the rapid acquisition of high-resolution dual-phase abdominal CTA which provides detailed information about the abdominal vascular structures [15].

On the other hand, Magnetic Resonance Imaging (MRI) has become an important tool for diagnosing brain pathologies and is increasingly widespread in veterinary medical practice [16]. Existing literature indicates that brain MRI findings are characterized by significant hyperintensity on T1 sequences in the lentiform nuclei of dogs and cats diagnosed with CPSS [11,16,17]. Similar MRI lesions have been observed in humans with chronic HE, and it is thought that these lesions are related to manganese accumulation [17]. Similar findings have also been documented in dogs [17]. Regarding with acute HE, more pronounced and more specific findings can be detected by MRI. In humans, findings such as diffusion restriction, widespread T2/FLAIR hyperintensities in cortex, and T2/FLAIR hyperintensities without any contrast agent accumulation in the thalamic nuclei have been described [18,19].

The aim of this study is to confirm the diagnosis of CPSS in cats and dogs using CTA and to comprehensively compare the clinical complaints of patients with brain MR findings.

MATERIAL AND METHODS

Ethical Statement

This study was approved by the Istanbul University-Cerrahpaşa, Faculty of Veterinary Medicine Animal Experiments Local Ethics Committee: 2024/02. Consent forms were obtained from all the owners of the patients who came to our clinic on those dates.

Data Collection

The data of our study were used from the images previously obtained from the Istanbul University, Veterinary Faculty, Department of Radiology between 2021 and 2023.

Animals

This study was conducted on animals applied to Animal Hospital of Istanbul University, Faculty of Veterinary Medicine between years 2021- 2023. All animals had the medical history, clinical symptoms, and biochemical values consistent with CPSS. A total of 9 animals, consisting of 5 dogs and 4 cats, were included in this study.

The patients included in the study consisted of cats and dogs of different breeds between the ages of 1-5 years.

Computed Tomography Protocol

Animals which were suspected of having CPSS underwent CTA. Haematological and serum biochemical parameters (Glucose, Creatinine, Urea, Urea/Creatinine, Phosphorus, Calcium, Total Protein, Albumin, Globulin, Alanine aminotransferase, Alkaline Phosphatase, Gamma-glutamyl transferase, Total bilirubin, Cholesterol, Ammonia, Amylase, Lipase) were measured before anaesthesia. Values were found between normal ranges. Furthermore, to confirm the diagnosis and gather more detailed information, brain MRI was performed on the animals. The HE scoring scale was converted from the scoring system previously used by Meyer [20]. In the evaluation of hepatic encephalopathy status, dogs with no clinical signs of hepatic encephalopathy were assigned grade 0; dogs with mild movement disorder, apathy or both were assigned grade 1; dogs with severe apathy, mild ataxia or both were assigned grade 2; dogs with hypersalivation, severe ataxia, head pressing, blindness, rotation or any combination of these signs were assigned grade 3; and dogs with seizures or in stupor or coma were assigned grade 4.

Patients were sedated using 5-7 mg/kg dose of propofol (Propofol-Genthon®) as premedication. Anesthesia was continued with 2% isoflurane (Isoflurane-Adeka®) after intubation.

The scans were conducted using 32-detector CT device (Siemens Somatom Go Now, Germany). All animals were scanned in a dorsal recumbent position. Initially, a topogram image was obtained to determine the scanning area. Subsequently, contrast medium (Opaxol TM) at a dose of 640 mg/kg and a rate of 3 mL/s was administered through a 20-24 gauge catheter via the right or left cephalic vein using a high-pressure injector pump. The threshold contrast enhancement value (100-120 HU) was set by manually marking the aortic lumen to trigger the start of the scan using the "bolus tracking" technique. The scan was automatically initiated when this threshold value was reached.

Arterial phase images were acquired from the caudal thoracic region to the pelvis with a 0.70 mm collimation, 1 mm slice thickness, and a table speed of 1.5 mm per gantry rotation. After the administration of contrast medium, a 30-40 sec delay was allowed, and portal phase images were obtained with the same collimation and slice thickness.

Dorsal, sagittal, maximum intensity projection (MIP), Multiplanar Reformat (MPR), and volume rendering images (VRT) were obtained from the acquired transverse images. Both transverse and reformatted images were evaluated by a radiologist experienced in abdominal radiology.

The MD-CT protocol is presented in detail below:

· Collimation: 16 x 0.75 mm
    - Section thickness: 1 mm
    - Reconstruction interval: 0.5 mm

· Tube voltage: 120 kV
    - Effective tube current: 160 mAs
    - Gantry rotation time: 650 msec
    - Scan direction: Cranio-caudal
    - Scan surface: 12-22cm
    - Scan time: 12-18 sec

MRI Examination

All magnetic resonance imaging was performed using a Siemens Magnetom Avanto scanner (Germany) with a magnetic field strength of 1.5 Tesla. For the imaging process, T1-weighted images were acquired with parameter settings of a repetition time (TR) of 350 ms and an echo time (TE) of 12 ms. The field of view for these images was set to 12 x 10 cm, and the matrix size was determined as 200 x 256. The slice thickness was set at 2.5 mm with a slice gap of 0.5 mm.

For the T2-weighted images, the TR and TE values were 3500 ms and 90 ms, respectively. The same field of view was used for these images, but the matrix size was adjusted to 320 x 284.

Enhanced T1-weighted images utilized a gadolinium-based contrast agent gadolinium DPTA (Gadovist-Bayer, Germany) 1.0 mmol/mL. This contrast agent was administered as an intravenous bolus at a dose of 0.1 mmol/kg.

This protocol was employed to ensure the highest image quality and optimal detection of diseases.

RESULTS

Summary of all cases have been shown in *Table 1*. A total of nine cases (5 dogs, 4 cats) were diagnosed with CPSS using CTA in this study. The population of dogs examined in this study consists of entirely small breeds. Seven of these cases, exhibited central nervous system symptoms, while only two cases did not exhibit any of these symptoms. Additionally, approximately 37% of the cases showed gastrointestinal symptoms (vomiting, diarrhea, excessive salivation).

| Table 1. *Summary of cases*									
Patient	Age	Species/ Breed	Body Weight (kg)	Vena Porta	Vena Hepatica	Shunt Type	Shunt Diameter	Grade for Hepatic Encephalopathy	Fasting NH_3 (µg/ dL)
Case 1	1 year	Dog/ Pekingese	8	Hipoplasic	Normal	Spleno-Caval (EHPSS)	4.8 mm	III	540
Case 2	5 months	Dog/Beagle	10	Hipoplasic	Hipoplasic	Spleno-Caval (EHPSS)	7.1 mm	III	180
Case 3	1 year	Cat/Mixed	3	Hipoplasic	Normal	Spleno-Caval (EHPSS)	4.6 mm	III	244
Case 4	5 years	Dog/Maltese terrier	5	Hipoplasic	Normal	Spleno-Caval (EHPSS)	3.6 mm	III	190
Case 5	7 months	Cat/ Siamesse	1.5	Hipoplasic	Normal	Mesenterico- Caval (EHPSS)	3.9 mm	III	290
Case 6	6 months	Cat/ Siamesse	2	Right portal vein branch is hypoplastic, left portal branch is ectatic	Normal	Between the left portal branch and the left hepatic vein (IHPSS)	5 mm	II	119
Case 7	4 years	Dog/ Yorkshire Terrier	3	Hipoplasic	Hipoplasic	Spleno-Caval (EHPSS)	6 mm	III	378
Case 8	1 year	Dog/ Pomerian	3	Normal	Normal	Between the left portal branch and the left hepatic vein (IHPSS)		0	198
Case 9	1.5 year	Cat/Scottish Fold	3	Hipoplasic	Normal	Porto-Caval Between the left portal vein and the vena cava caudalis (IHPSS)	4.8 mm	IV	325
Reference value: 23-78 µg/dL (for cats), 16-75 µg/dL (for dog)									
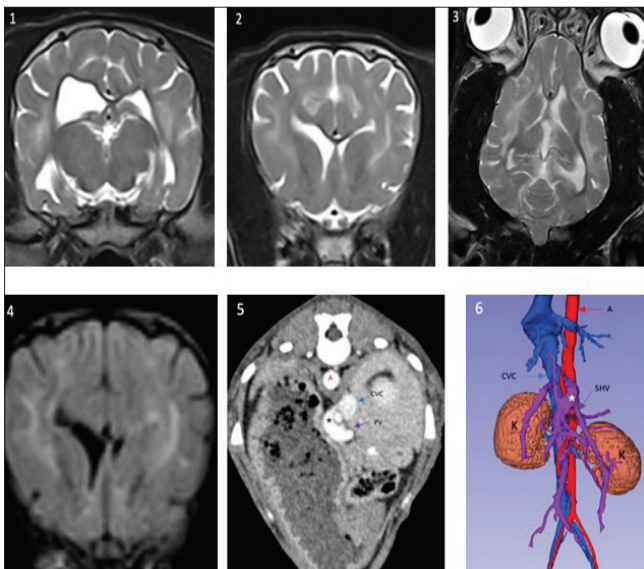
Fig 1. MRI and CT findings of case 2. 1-2: Tranversal and 3: dorsal-T2-weighted MR image showing combined symmetric hyperintensity *(arrows)* in the white matter of the brain, 4: transversal FLAIR MR image showing bilateral and symmetric hyperintensity *(arrows)* affecting the periventricular white matter, 5: transversal CTA showing vascular connection *(asterisk)* between the splenic vein (SHV) and the vena cava caudalis (CVC), (A: Aorta), 6: dorsoventral 3D reconstruction image showing the shunt vessel between CVC and splenic vein

Fig 2. MRI and CT findings of case 9. 1: Transversal T2 W MR image (T) shows hypersensitivity in the thalamus, 2: Transversal T2 W MR image (RF) shows hypersensitivity in the reticular formation, 3: Dorsoventral 3D reconstruction CT image showing the shunt vessel *(asterisk)* between the left branch of the vena porta in the intra hepatic section (IH) and the vena cava caudalis, 4: Lateral CT image showing the shunt connection of the vena porta with the vena cava caudalis *(asterisk)* 5-6: MR imaging after the patient was treated shows that the hypersensitivity in the thalamus and reticular formation decreased (A: Aorta)

The diagnosis of EHPS was observed in six cases (case 1, 2, 3, 4, 5, 7) *(Table 1)*. Five of these cases displayed spleno-caval shunt profiles, while one (case 5) showed a mesenterico-caval shunt profile according to Nelson & Nelson's new morphological decriptions [4]. In case 5 with a mesenterico-caval shunt profile, it was determined that the vena mesenterica caudalis joined the vena cava caudalis (VCC) at the level of L4 vertebra and VCC was dublicated. Five of these cases (case 1, 3, 4, 5, 7) showed atrophic changes such as sulcal and ventricular expansion and a decrease in gyrus volume in the brain. In the brain MRI of case 2, increased signal intensity was observed on T2-weighted and fluid-attenuated inversion recovery (FLAIR) sequences of the periventricular white matter regions *(Fig. 1)*. It was determined that all cases diagnosed with EHPS had hypoplastic vena porta.

The diagnosis of IHPS was observed in three cases (case 6, 8, 9) *(Table 1)*. In all of these cases, the integration of left portal vein with VCC was observed. Brain MRI evaluations of these cases revealed the followings: in case 8 (HE grade: 0), no pathological findings were found, while in case 9, significant hyperintense signal changes were detected on T2-weighted, FLAIR, and diffusion-weighted imaging (DWI) sequences in the specific regions of the central nervous system (i.e. pons, mesencephalon, bilateral cerebral peduncles, and bilateral thalamus) *(Fig. 2)*. This patient (case 9) also showed compulsive circling behaviours. Case 6 had a signal increase on T1-weighted image in the lentiform nucleus.
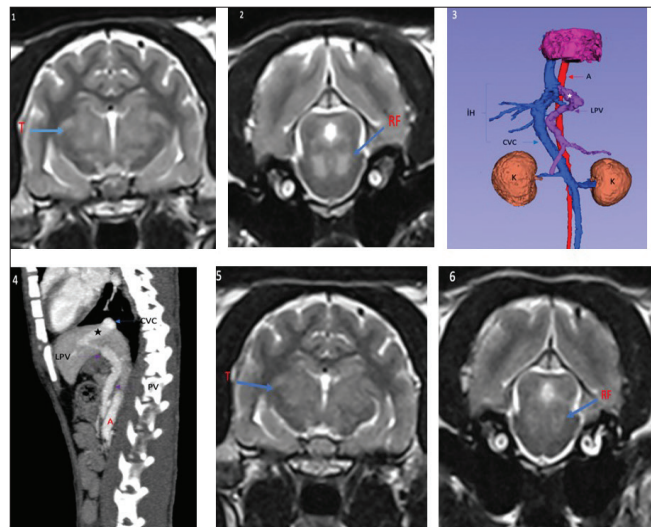
In our study, elevated ammonia concentrations were detected in a significant portion of the participants, surpassing the reference values. With in the scope of this study, there is no evidence of any shunt existence between the portal vein and azygos vein.

DISCUSSION

PSS which causes ammonia-rich blood to bypass away from the liver is one of the main factors contributing to the development HE in dogs and cats. This mechanism led to significant hyperammonemia in some of the animals included in our study.

Hyperammonemia can lead to irreversible damage in the developing brain, such as cortical atrophy, ventricular expansion, demyelination, or hypodensities in gray and white matter. Many studies in humans have reported that acute hepatic or hyperammonemic encephalopathy is considered one of the causes of cortical laminar necrosis, and these effects are reported to be particularly severe in neonatal onset [21-23]. Different pathogenic mechanisms have been shown to be involved, including changes in cerebral energy metabolism [21,24]. In two separate case reports by Spinillo et al.[25] and Moon et al.[26] two dogs had MRI findings of diffuse bilateral symmetric hyperintense signals on T2-weighted in the cerebral cortex. Different images taken at various times in the same studies reported the brain atrophy due to cortical laminar necrosis [20,26]. This corresponds to the brain atrophy symptoms we observed in five out of the nine animals in our study.

However, it is possible to say that this occurred especially as a result of acute hyperammonemia and progressed to chronic effects such as brain atrophy over time. Four of the cases with brain atrophy had spleno-caval shunts in CTA, and one case had a mesenterico-caval shunt (case 5).

Based on CTA findings obtained from the dog (case 2), a diagnosis of EHPS (spleno-caval) was made. On MRI examination, minimal ectasia of the third and lateral ventricles was observed. Remarkably, significant signal intensity increases were observed on T2-weighted and FLAIR sequences in the periventricular white matter of both the left and right hemispheres. However, no pathological contrast fixation was observed after applying intravenous contrast agent.

Human studies have reported that periventricular white matter involvement is observed in acute HE [27-30]. In a more comprehensive study involving 101 human patients, the periventriculer white matter involvement which was devoloped as secondary to acute HE was reported as the most third common finding in MRI [28]. The exact etiology of this condition, in which specific regions of the white matter are affected, is not yet fully understood. Specific areas in white matter regions of the corticospinal pathway or nearby might be more vulnerable to develop secondary edema after liver failure. The underlying reasons for this vulnerability have not yet been definitively understood, but it is thought that the mechanisms such as energy deficiencies or abnormal expression of glutamate transporters might be involved [30].

In our cases which were diagnosed with EHPS, portal vein hypoplasia was observed and were rated as grade III according to Meyer's HE classification [21]. We cosidered that the portal vein volume and PSS volume might have been related to the patient's clinical condition.

Among the brain MRI features of PSS, hyperintensity is prominent on T1-weighted imaging within the lentiform nuclei. These lesions are isointense on T2 and do not show any contrast uptake [11,20]. It is known that these findings regress after PSS repair. Similar lesions have been observed in humans with chronic HE [31].

High manganese concentrations have been found in both blood [32-35] and brain tissues [36,37] of cats and dogs. The literature suggests that manganese accumulation can cause an increase in T1-weighted signal intensity in the lentiform nucleus [15,38]. Although an increase in T1-weighted signal intensity in the lentiform nucleus is the most common finding, it was only observed in one of the cases which were diagnosed as IHPS (case 6) in our study. Since manganese values were not measured in our study, the relationship with our findings could not be evaluated. Among our cases with IHPSs, one dog (case 8; HE grade: 0) did not show any pathological changes in the brain MRI.

Based on the CTA findings of our 1-year-old cat (case 9), a diagnosis of IHPS (between the left portal branch and the VCC) was made. Brain MRI examination revealed significant hyperintense signal intensity changes on T2-weighted, FLAIR, and DWI sequences in the Pons, mesencephalon, cerebral peduncles, and thalamus. These findings were considered to reflect a combination of vasogenic and cytotoxic edema. However, no pathological contrast accumulation was observed. A notable point is that rostral thalamic lesions can lead to compulsive circling behavior in cats [39]. In our study, compulsive circling behaviour was present in cats with thalamic lesions. In addition, a study based on a rat model showed that glucose metabolism was increased maximally in the reticular formation after PSS development, and consequently, caused the development of hyperammonemia [40]. Similar to this, significant hyperintense lesions were observed in the reticular formation in two West Highland White Terrier dogs with PSS [41].

The brain MRI findings of Case 9 such as increased T2A signal in the thalamus and mesencephalon were similar to lesions caused by thiamine deficiency [42]. However, a specific analysis of thiamine levels could not be performed in this current study. The patient's balanced diet and no consumption of supplementary food indicate that thiamine deficiency was not diet-related [43]. A decrease in bile production and consequent digestive and absorption problems may occur as a result of deterioration of liver functions in patients with PSS [44]. Thiamine is stored in liver and play an important role as a co-enzyme in carbohydrate metabolism. Thiamine deficiency can lead to symptoms similar to HE, such as Wernicke's encephalopathy [45]. It should be taken into account that thiamine deficiency may be a potential factor, especially in intestinal malabsorptive states or other chronic enteropathies, which may reduce the absorption of thiamine from the diet.

However, there is no specific evidence of thiamine deficiency or similar brain pathologies in patients with PSS [11,20,28,46]. As a clinical approach in our study, medical treatment and dietary protocol were applied since the patient's owner refused the surgical intervention. B-complex vitamin preparations were added to this treatment. After six months of follow-up, a decrease in the lesions was observed in the patient's brain MRI. In the light of these observations, it is difficult to directly associate these findings with thiamine deficiency or PSS.

In this study, various brain MRI findings were observed in the cases with PSS. Despite methodological similarities, studies on animal models with PSS yield different results and findings. In our study, we also observed findings that reflect the diversity encountered in the literature. However, detailed studies directly comparing shunt type with clinical and MRI findings in animals with PSS are

limited. Within the scope of this study, we examined the potential relationships between the type of PSS and brain MRI findings. With new studies, it will allow a more precise identification of potential lesions in the brain that may be associated with the type of shunt.

DECLARATIONS

REFERENCES

1. Anglin EV, Lux CN, Sun X, Folk CA, Fazio C: Clinical characteristics of prognostic factors for, and long-term outcome of dogs with multiple acquired portosystemic shunts: 72 cases (2000-2018). *J Am Vet Med Assoc,* 260 (S1): S30-S39, 2021. DOI: 10.2460/javma.20.12.0703

2. Saravanan M, Ramkumar PK: Diseases of hepatobiliary system of dogs and cats. **In,** Rana T (Ed): Introduction to Diseases, Diagnosis, and Management of Dogs and Cats. 377-393, Academic Press, 2024.

3. Plested MJ, Zwingenberger AL, Brockman DJ, Hecht S, Secrest S, Culp WTN, Drees R: Canine intrahepatic portosystemic shunt insertion into the systemic circulation is commonly through primary hepatic veins as assessed with CT angiography. *Vet Radiol Ultrasound,* 61 (5): 519-530, 2020. DOI: 10.1111/vru.12892

4. Humphreys WJ, Sumping JC, Maddox TW, Marwood R: Enlargement of the hepatic artery is present in dogs with a congenital extrahepatic portosystemic shunt and is independent of shunt insertion into the systemic circulation. *Vet Radiol Ultrasound,* 65, 149-156, 2024. DOI: 10.1111/vru.13329

5. Lidbury JA, Cook AK, Steiner JM: Hepatic encephalopathy in dogs and cats. *J Vet Emerg Crit Care,* 26 (4): 471-487, 2016. DOI: 10.1111/vec.12473

6. Windsor RC, Olby NJ: Congenital portosystemic shunts in five mature dogs with neurological signs. *J Am Anim Hosp Assoc,* 43 (6): 322-331, 2007. DOI: 10.5326/0430322

7. Butterworth RF: Pathophysiology of hepatic encephalopathy: A new look at ammonia. *Metab Brain Dis,* 17 (4): 221-227, 2002. DOI: 10.1023/a:1021989230535

8. Konstantinidis AO, Adamama-Moraitou KK, Patsikas MN, Papazoglou LG: Congenital portosystemic shunts in dogs and cats: Treatment, complications and prognosis. *Vet Sci,* 10 (5): 346, 2023. DOI: 10.3390/vetsci10050346

9. Jaffe A, Lim JK, Jakab SS: Pathophysiology of hepatic encephalopathy. *Clin Liver Dis,* 24 (2): 175-188, 2020. DOI: 10.1016/j.cld.2020.01.002

10. Williams A, Gow A, Kilpatrick S, Tivers M, Lipscomb V, Smith K, Day MO, Jeffery N, Mellanby RJ: Astrocyte lesions in cerebral cortex and cerebellum of dogs with congenital ortosystemic shunting. *J Vet Sci,* 21 (3):e44, 2020. DOI: 10.4142/jvs.2020.21.e44

11. Konstantinidis AO, Patsikas MN, Papazoglou LG, Adamama-Moraitou KK: Congenital portosystemic shunts in dogs and cats:

Classification, pathophysiology, clinical presentation and diagnosis. *Vet Sci,* 10 (2):160, 2023. DOI: 10.3390/vetsci10020160

12. Atasoy B, Alkan A: Metabolic and toxic paediatric brain disorders. *Trd Sem,* 7 (3): 306-323, 2019.

13. Kim, SE, Giglio RF, Reese DJ, Reese SL, Bacon NJ, Ellison GW: Comparison of computed tomographic angiography and ultrasonography for the detection and characterization of portosystemic shunts in dogs. *Vet Radiol Ultrasound,* 54 (6): 569-574, 2013. DOI: 10.1111/vru.12059

14. Atasoy C, Akyar S: Multidetector CT: Contributions in liver imaging. *Eur J Radiol,* 52 (1): 2-17, 2004. DOI: 10.1016/j.ejrad.2004.03.029

15. Laitinen MR, Matheson JS, O'Brien RT: Novel technique of multislice CT angiography for diagnosis of portosystemic shunts in sedated dogs. *Open Vet J,* 3, 115-120, 2013. DOI: 10.4236/ojvm.2013.32019

16. Fernandes R, Driver C, Rose JH, Rusbridge C: MRI findings in two West Highland White Terrier dogs with hepatic encephalopathy secondary to portosystemic shunt. *Vet Rec Case Rep,* 7 (3):e000814, 2019. DOI: 10.1136/vetreccr-2019-000814

17. Torisu S, Washizu M, Hasegawa D, Orima H: Measurement of brain trace elements in a dog with a portosystemic shunt: Relation between hyperintensity on T1-weighted magnetic resonance images in lentiform nuclei and brain trace elements. *J Vet Med Sci,* 70 (12): 1391-1393, 2008. DOI: 10.1292/jvms.70.1391

18. Denk CH, Kunzmann J, Maieron A, Wöhrer A, Quinot V, Oberndorfer S: Histopathological examination of characteristic brain MRI findings in acute hyperammonemic encephalopathy: A case report and review of the literature. *Neuroradiol J,* 1:19714009231212370, 2023. DOI: 10.1177/19714009231212370

19. Rosario M, McMahon K, Finelli PF: Diffusion-weighted imaging in acute hyperammonemic encephalopathy. *Neurohospitalist,* 3 (3): 125-130, 2013. DOI: 10.1177/1941874412467806

20. Meyer HP, Legemate DA, van den Brom W, Rothuizen J: of chronic hepatic encephalopathy in dogs by the benzodiazepine-receptor partial inverse agonist sarmazenil, but not by the antagonist flumazenil. *Metab Brain Dis,* 13 (3): 241-251, 1998. DOI: 10.1023/a:1023228126315

21. Choi JM, Kim YH, Roh SY: Acute hepatic encephalopathy presenting as cortical laminar necrosis: case report. *Korean J Radiol,* 14 (2): 324-328, 2013. DOI: 10.3348/kjr.2013.14.2.324

22. Arnold SM, Els T, Spreer J, Schumacher M: Acute hepatic encephalopathy with diffuse cortical lesions. *Neuroradiology,* 43 (7): 551-554, 2001. DOI: 10.1007/s002340000461

23. Braissant O, McLin VA, Cudalbu C: Ammonia toxicity to the brain. *J Inherit Metab Dis,* 36 (4): 595-612, 2013. DOI: 10.1007/s10545-012-9546-2

24. Braissant O: Ammonia toxicity to the brain: Effects on creatine metabolism and transport and protective roles of creatine. *Mol Genet Metab,* 1, 53-58, 2010. DOI: 10.1016/j.ymgme.2010.02.011

25. Spinillo S, Golini L, Motta L: Brain MRI findings in a dog with late onset epileptic seizure after portosystemic shunt attenuation. *Vet Rec Case Rep,* 8 (3):e001159, 2020. DOI: 10.1136/vetreccr-2020-001159

26. Moon SJ, Kim JW, Kang BT, Lim CY, Park HM: Magnetic resonance imaging findings of hepatic encephalopathy in a dog with a portosystemic shunt. *J Vet Med Sci,* 74 (3): 361-366, 2012. DOI: 10.1292/jvms.11-0198

27. White RN, Parry AT: Morphology of congenital portosystemic shunts involving the right gastric vein in dogs. *J Small Anim Pract,* 56 (7): 430-440, 2015. DOI: 10.1111/jsap.12355

28. Özütemiz C, Roshan SK, Kroll NJ, Benson JC, Rykken JB, Oswood MC, Zhang L, McKinney AM: Acute toxic leukoencephalopathy: Etiologies, imaging findings, and outcomes in 101 patients. *AJNR,* 40 (2): 267-275, 2019. DOI: 10.3174/ajnr.A5947

29. de Oliveira AM, Paulino MV, Vieira APF, McKinney AM, da Rocha AJ, Dos Santos GT, Leite CDC, Godoy LFS, Lucato LT: Imaging patterns of toxic and metabolic brain disorders. *Radiographics,* 39 (6): 1672-1695, 2019. DOI: 10.1148/rg.2019190016

30. Alonso J, Córdoba J, Rovira A: Brain magnetic resonance in hepatic encephalopathy. *Semin Ultrasound CT MR,* 35 (2): 136-152, 2014. DOI: 10.1053/j.sult.2013.09.008

31. Wisner E, Zwingenberger A: Atlas of Small Animal CT and MRI. John Wiley & Sons, 2015.

32. Krieger D, Krieger S, Jansen O, Gass P, Theilmann L, Lichtnecker H: Manganese and chronic hepatic encephalopathy. *Lancet,* 346 (8970): 270-274, 1995. DOI: 10.1016/s0140-6736(95)92164-8

33. Fukuzawa T, Matsutani S, Maruyama H, Akiike T, Saisho H, Hattori T: Magnetic resonance images of the globus pallidus in patients with idiopathic portal hypertension: a quantitative analysis of the relationship between signal intensity and the grade of portosystemic shunt. *J Gastroenterol Hepatol,* 21 (5): 902-907, 2006. DOI: 10.1111/j.1440-1746.2006.04226.x

34. Long LL, Li XR, Huang ZK, Jiang YM, Fu SX, Zheng W: Relationship between changes in brain MRI and (1)H-MRS, severity of chronic liver damage, and recovery after liver transplantation. *Exp Biol Med (Maywood),* 234 (9): 1075-1085, 2009. DOI: 10.3181/0903-RM-118

35. Spahr L, Vingerhoets F, Lazeyras F, Delavelle J, DuPasquier R, Giostra E, Mentha G, Terrier F, Hadengue A: Magnetic resonance imaging and proton spectroscopic alterations correlate with parkinsonian signs in patients with cirrhosis. *Gastroenterology,* 119 (3): 774-781, 2000. DOI: 10.1053/gast.2000.17857

36. Rose C, Butterworth RF, Zayed J, Normandin L, Todd K, Michalak A, Spahr L, Huet PM, Pomier-Layrargues G: Manganese deposition in basal ganglia structures results from both portal-systemic shunting and liver dysfunction. *Gastroenterology,* 117 (3): 640-644, 1999. DOI: 10.1016/s0016-5085(99)70457-9

37. Klos KJ, Ahlskog JE, Kumar N, Cambern S, Butz J, Burritt M, Fealey RD, Cowl CT, Parisi JE, Josephs KA: Brain metal concentrations in chronic liver failure patients with pallidal T1 MRI hyperintensity. *Neurology,* 67 (11): 1984-1989, 2006. DOI: 10.1212/01.wnl.0000247037.37807.76

38. Gow AG, Marques AI, Yool DA, Duncan A, Mellanby RJ: Whole blood manganese concentrations in dogs with congenital portosystemic shunts. *J Vet Intern Med,* 24 (1): 90-96, 2010. DOI: 10.1111/j.1939-1676.2009.0408.x

39. Quesnel AD, Parent JM: Cat with signs of neurological disease. **In**, Rand J (ed): Problem-Based Feline Medicine. 795-820, Saunders, 2009.

40. Lockwood AH, Ginsberg MD, Rhoades HM, Gutierrez MT: Cerebral glucose metabolism after portacaval shunting in the rat: Patterns of metabolism and implications for the pathogenesis of hepatic encephalopathy. *J Clin Invest,* 78 (1): 86-95, 1986. DOI: 10.1172/JCI112578

41. Fernandes R, Driver C, Rose JH, Rusbridge C: MRI findings in two West Highland White Terrier dogs with hepatic encephalopathy secondary to portosystemic shunt. *Vet Rec Case Rep,* 7 (3):e000814, 2019. DOI: 10.1136/vetreccr-2019-000814

42. Moon SJ, Kang MH, Park HM: Clinical signs, MRI features, and outcomes of two cats with thiamine deficiency secondary to diet change. *J Vet Sci,* 14 (4): 499-502, 2013. DOI: 10.4142/jvs.2013.14.4.499

43. Kritikos G, Parr JM, Verbrugghe A: The role of thiamine and effects of deficiency in dogs and cats. *Vet Sci,* 4 (4):59, 2017. DOI: 10.3390/vetsci4040059

44. Albrecht J, Faff L: Astrocyte-neuron interactions in hyperammonemia and hepatic encephalopathy. **In,** Felipo V, Grisolia S (Eds): Hepatic Encephalopathy, Hyperammonemia, and Ammonia Toxicity. 45-54, Springer, US,1994.

45. Markovich JE, Heinze CR, Freeman LM: Thiamine deficiency in dogs and cats. *J Am Vet Med Assoc,* 243 (5): 649-656, 2013. DOI: 10.2460/javma.243.5.649

46. Carrera I, Kircher PR, Meier D, Richter H, Beckman K, Dennler M: In vivo proton magnetic resonance spectroscopy for the evaluation of hepatic encephalopathy in dogs. *Am J Vet Res,* 75 (9): 818-827, 2014. DOI: 10.2460/ajvr.75.9.818